

# Preparation of Functional Long-Subchain Hyperbranched Polystyrenes via Post-polymerization Modification: Study on the Critical Role of Chemical Stability of Branching Linkage

Mo Zhu,<sup>[a]</sup> Nairong Hao,<sup>\*[a]</sup> Muhammad Zaheer,<sup>[a]</sup> Jinxian Yang,<sup>[b]</sup> and Lianwei Li<sup>\*[b]</sup>

Post-polymerization modification (PPM) is one of the most powerful strategy for preparing polymers with functional groups that cannot be synthesized by direct polymerization. So far, numerous experimental efforts have been devoted to the stability issue of monomer structures during the PPM process, but little attention was paid to chemical linkages. However, for hyperbranched polymers, a minor change of linkage unit could lead to a significant influence on the overall stability and performance of polymer materials. In this work, we investigated the chemical stability of long-subchain hyperbranched polystyr-

enes with ester, aryl ether, and carbon-carbon bonds as branching linkages under a few most popular PPM conditions, including NaOH hydrolysis reaction, TFA-promoted hydrolysis reaction, BBr<sub>3</sub>-catalyzed methoxy-hydroxyl conversion reaction, and LiAlH<sub>4</sub> carbonyl reduction reaction. Related results are summarized into a synthetic route map that can provide practical and intuitive guidance for preparing functional long-subchain hyperbranched polystyrenes and other type of polymers by PPM for future applications.

## 1. Introduction


Post-polymerization modification (PPM) is one of the most powerful synthetic approaches to produce functional materials based on the limited types of polymerization methods. In the past few decades it has attracted great interest from both academia and industry, which is because it is not only able to facilitate the preparation of functional polymers that cannot be prepared by direct polymerization of the corresponding functional monomers, but also to accelerate the discovery of novel combinatorial materials.<sup>[1]</sup> So far, many chemical transformations have been used for the PPM process, such as active ester exchange, thiol exchange, Michael-addition, metal-catalyzed cross-coupling, thiol-ene, thiol-yne and the Huisgen 1,3-dipolar cycloaddition reactions, to name but a few.<sup>[2,3]</sup> It is no exaggeration to say that the post-polymerization modification approach has been correlated with all aspects of polymer science from fundamental study to industrial application.


During the PPM process, one main issue normally needs to consider is the stability of polymer precursor and polymer product under various PPM conditions. So far, numerous research works have indicated that the thermal and chemical stability of polymer backbone and side chains are extremely important for the application of functional polymer materials.<sup>[4–18]</sup> For example, Hammond et al. found that the chemical stability of polymers for lithium-air battery application is related with the electron-withdrawing property of functional groups on the polymer side chain.<sup>[10]</sup> Bae et al. systematically studied the alkaline stability of polymer backbones for anion exchange membrane application, and suggested that the use of all carbon-based polymer repeating units, instead of polymers bearing aryl ether bonds, can significantly enhance long-term alkaline stability;<sup>[14]</sup> recently, Elabd et al. found that the alkaline stability of polymerized ionic liquids has no correlation to that of their analogous small molecule ionic salts, highlighting the fact that even the model study on small molecules may not provide a solid basis for evaluating stability of polymers.<sup>[11,13]</sup> These studies also questioned the stability issue of polymer backbones during the PPM process.

In addition to the stability issue of monomer structures, the stability issue of chemical linkages is the other main concern. This is because a minor change of linkage unit could lead to a significant influence on the overall stability and performance of polymer materials.<sup>[4–9,15,18]</sup> Namely, Itoh et al. found that the alteration of branching linkage of branched poly(ethylene oxide) (PEO) from ester to ether significantly enhances the alkaline chemical stability and ionic conductivity of the composite solid polymer electrolytes for battery application;<sup>[19]</sup> Rice et al. found that the type of chemical linkage on PEO dramatically influences the in vivo gene transfer efficiency;<sup>[7]</sup> Ein-Eli et al. found that the sulfone linkage has a profound

[a] M. Zhu, N. Hao, M. Zaheer  
Department of Chemical Physics  
University of Science and Technology of China  
Hefei (China)  
E-mail: hnr@mail.ustc.edu.cn

[b] Dr. J. Yang, Prof. Dr. L. Li  
College of Chemistry and Environmental Engineering  
Shenzhen University  
Shenzhen (China)  
E-mail: lianweili@szu.edu.cn

 Supporting information for this article is available on the WWW under <https://doi.org/10.1002/open.202000143>

 © 2020 The Authors. Published by Wiley-VCH GmbH. This is an open access article under the terms of the Creative Commons Attribution Non-Commercial NoDerivs License, which permits use and distribution in any medium, provided the original work is properly cited, the use is non-commercial and no modifications or adaptations are made.

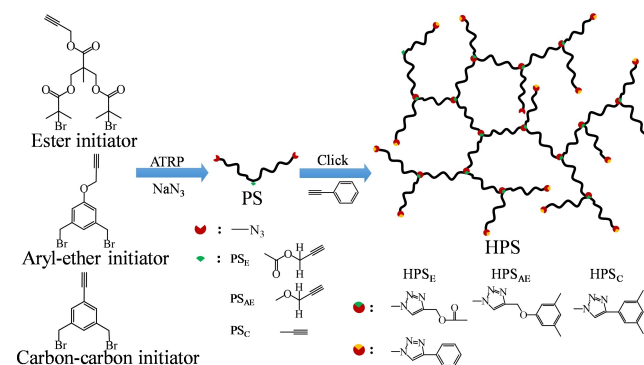
negative influence on the thermal and alkaline stability of anion exchange polymer membranes;<sup>[8]</sup> Hillmyer et al. clarified that the urethane linkages actually could provide a good chemical stability of PDMS-urethane polymers.<sup>[9]</sup> In addition, the linkage stability also significantly affects the properties such like the controlled release of responsive polymeric assemblies,<sup>[15]</sup> the degradation and reuse of thermosetting engineering polymers,<sup>[18]</sup> and the fabrication of high performance photo-voltaic devices.<sup>[16]</sup> However, the critical role of linkage unit is very easy to be overlooked because it generally accounts for only a small fraction (1%~5%) of entire constituting units for a given functional polymer.

Long-subchain hyperbranched polymers (LHPs) with long linear chains between every two branching points have received considerable attention in the past two decades, since it can combine the excellent mechanical properties of linear polymers with the special physical properties of hyperbranched polymers. Three main methods have been reported to synthesize LHPs: (1)  $A_2 + B_3$  approach,<sup>[20,21]</sup> (2) self-condensing vinyl polymerization (SCVP) approach,<sup>[22,23]</sup> and (3) macromonomer  $AB_n$  approach.<sup>[24–32]</sup> In vein of the  $A_2 + B_3$  approach, Long et al. synthesized a series of LHPs such as hyperbranched poly(ether ester)s, and polysulfone ionomers by polycondensation of an  $A_2$  chain and a  $B_3$  monomer.<sup>[21]</sup> Alternatively, Gao et al.<sup>[22]</sup> synthesized hyperbranched poly(tertiary amino methacrylate)s with hydrophilic core and hydrophobic shell via SCVP methodology. However, neither of the above two synthesis methods could offer little control over chain parameters. As for the macromonomer-based step-growth polymerization strategy, the polymerization of the  $AB_n$  functionalized macromonomer has shown much better control over the chain parameters for LHPs, such as the average branching subchain length and the subchain length distribution. These two parameters are regarded as the first two considerations when we address the structure-property relationship for LHPs, because they are related to the basic properties of LHPs in solution and the bulk phase.

So far, a number of examples have been reported to construct hyperbranched systems via  $AB_n$  macromonomer approach. Namely, Hutchings et al. adopted this  $AB_2$  macromonomer approach to construct a number of LHPs model systems<sup>[24,25]</sup> by the Williamson coupling reaction, and they established a few structure-property relationships about the rheological properties and the phase behavior of LHPs; Our group synthesized LHPs with controllable branched subchain length by using the seesaw-type macromonomer.<sup>[26–28]</sup> In addition, we synthesized the  $AB_n$  ( $n \geq 2$ ) LHPs with  $AB_n$  ( $n \geq 2$ ) macromonomer for the first time, and studied the relationship between branching pattern and solution properties.<sup>[29,30]</sup> It is worth mentioning that in our recent work,  $AB_2$  hyperbranched polystyrenesulfonate were successfully synthesized by soft sulfonation with acetyl sulfate as the sulfonating reagent, using  $AB_2$  hyperbranched polystyrene with total carbon branching linkage as the precursor.<sup>[31]</sup> The results clearly prove that the total carbon branching linkage has an incomparable stability advantage over ester linkage under the condition of sulfonated PPM, indicating that the stability of the branch point in the PPM process is very important.

The combination of atom transfer radical polymerization (ATRP) and azide-alkyne cycloaddition coupling reaction has been widely for the construction of LHPs in related studies.<sup>[32,33]</sup> To gain functional macromonomers with reactive moieties, alkyne and azido groups are generally introduced into the initiator structure at the beginning via esterification or Williamson reactions,<sup>[27,32]</sup> which unavoidably introduces ester-based or ether-based 1,2,3-Triazole (TA) linkage into the branching point in the final LHPs. Without doubt, the existence of labile linkages could be fatal under various PPM conditions. Obviously, the greatest challenge lies in the stability issue of branching linkages under PPM condition, because they typically possess a poorer chemical stability compared with the repeating units. Although the stability of the ester and ether bonds in small molecules has been studied clearly, the stability of the ester and ether bonds incorporated in the hyperbranched polymer, which might be different from the corresponding small molecules, is still unknown. In fact, the stability of the ester bond and ether bond at the branching point is not only affected by the electron-withdrawing effect of the 1,2,3-triazole ring spaced by a methylene group, but also by the tension of the branching point caused by the segment motion of the branched chain. Therefore, it is necessary to explore the stability of branching points under real experimental conditions.

In this work, we extend to study the chemical stability of polystyrene LHPs with different branching linkages under various PPM conditions to gain the guide map for the preparation of functional hyperbranched polystyrenes for different applications purposes. Considering that the stability of a given type of chemical linkage might be different between small molecular and macromolecular systems due to the potential difference in steric effect or local hydrophobic/hydrophilic property, the direct construction of macromolecular systems is a must for the accurate evaluation of the stability of chemical linkage. For our purpose, the aryl-ether (AE), ester (E), and carbon-carbon (C) linkage are designed into the branching points of hyperbranched polystyrenes, respectively (Scheme 1). With three model hyperbranched polystyrenes with different branching linkages ( $HPS_{AE}$ ,  $HPS_E$  and  $HPS_C$ ) in hand, we aim to get insight into the optimal linkage structure under different PPM conditions for specific application purposes in future.



**Scheme 1.** Schematic illustration of the topological structures of long-subchain hyperbranched polystyrenes with ester ( $HPS_E$ ), aryl-ether ( $HPS_{AE}$ ) and carbon-carbon ( $HPS_C$ ) linkages.

## 2. Results and Discussion

### 2.1. Preparation and Characterization of HPS<sub>AE</sub>, HPS<sub>E</sub> and HPS<sub>C</sub> Hyperbranched Samples

In this study, three AB<sub>2</sub>-type ATRP initiators with the ester (E), aryl-ether (AE) and carbon (C) linkages are designed. The synthetic schemes are summarized in Scheme S1. The <sup>1</sup>H NMR characterization confirms the chemical structures of resultant initiators (Figure S1). The styrene monomer conversion of ATRP process was controlled to be below 60% to maintain high chain-end functionality. The three polystyrene macromonomers all show small dispersities ( $M_w/M_n$ ) between 1.10 and 1.12, indicating a good control over polymerization process, and their molar mass information is summarized in Table S1. For the convenience of discussion, the three macromonomers are denoted as PS<sub>E</sub>, PS<sub>AE</sub> and PS<sub>C</sub>, where the subscripts "E", "AE" and "C" represent the abbreviations for "ester", "aryl-ether" and "carbon", respectively. Specifically,  $M_n$  is determined to be  $\sim 1.80 \times 10^4$ ,  $\sim 8.70 \times 10^3$  and  $\sim 7.90 \times 10^3$  g/mol for PS<sub>E</sub>, PS<sub>AE</sub> and PS<sub>C</sub>, respectively.

The preparation of alkyne/azide functionalized macromonomers is achieved via a bromine/azide substitution reaction in DMF. The azide/alkyne click chemistry was utilized to prepare highly polydispersed hyperbranched polystyrenes (HPS<sub>AE</sub>, HPS<sub>E</sub> and HPS<sub>C</sub>). The structural details for these alkyne/azide functionalized macromonomers and LHPs were confirmed by <sup>1</sup>H NMR characterization (Figure 1). Besides the broad aromatic and aliphatic regions of styrene monomer, the feature signals (H<sub>a</sub>, H<sub>b</sub> and H<sub>c</sub>) which could reflect the success of click coupling are also studied. As shown in Figure 1a, the signals for proton H<sub>a</sub>, H<sub>b</sub> and H<sub>c</sub> change from 2.31 to 7.70 ppm, 4.55 to 4.92 ppm, and 3.92 to 5.05 ppm after click reaction, respectively, signifying the formation of triazole ring. Similar spectra were also observed for HPS<sub>AE</sub> and HPS<sub>C</sub> (Figures 1b and 1c).

To avoid to possible influence from the residual azide groups on the periphery of individual hyperbranched chains during the stability study, phenylacetylene is used to end-cap the azide group to form stable triazole group. The consumption of azide moiety is confirmed via the disappearance of asymmetric vibration of azide group at  $2100\text{ cm}^{-1}$  in FTIR spectra (Figure 2a). Figure 2b further displays the SEC curves of three hyperbranched samples, and their molar mass information is summarized in Table S2. It is worth noting that the adopted AB<sub>2</sub> macromonomer strategy precisely ensures that each branching point contains only one functional linkage.

### 2.2. Stability of Branching Linkage toward Alkaline Hydrolysis.

The first typical type of PPM condition we studied is the alkaline hydrolysis because it is one of the most widely used PPM condition for the preparation of a variety of functional polyelectrolytes which are not easily accessible via direct polymerization method, such as poly(acrylic acid) (PAA),<sup>[34,35]</sup> polystyrolsulfonate (PSS),<sup>[36]</sup> poly(ethylene imine) (PEI),<sup>[37]</sup> and

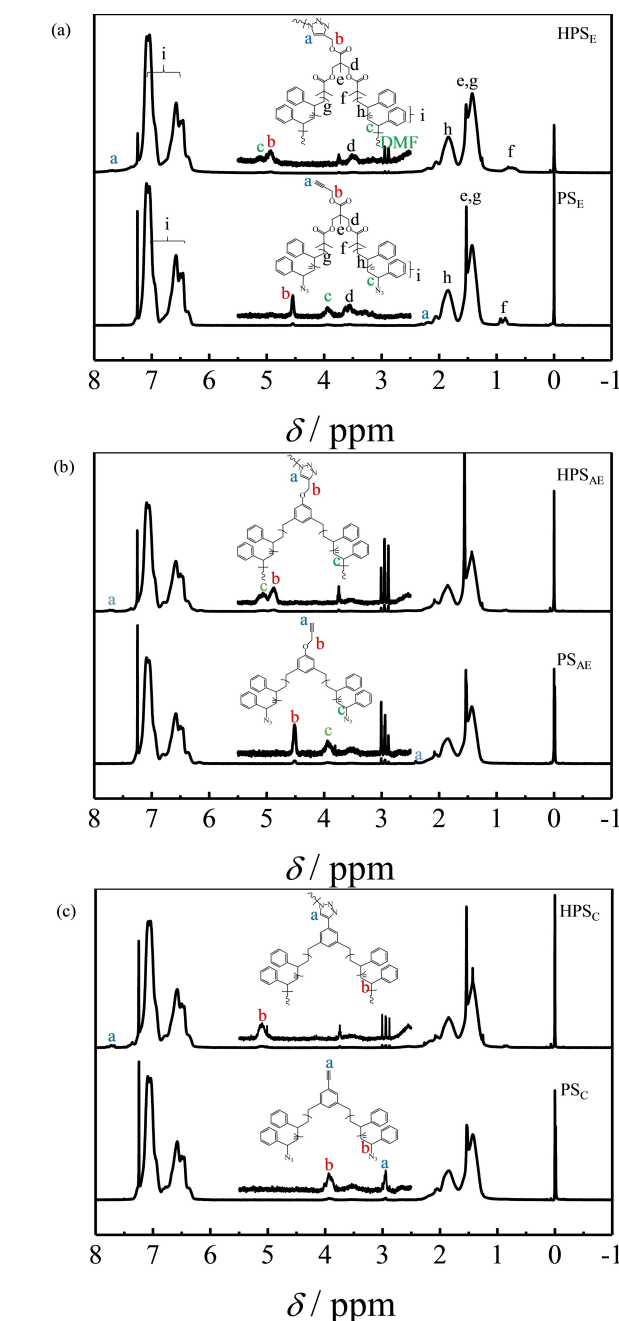


**Figure 1.** <sup>1</sup>H NMR spectra of alkyne/azide functionalized AB<sub>2</sub> macromonomers and corresponding hyperbranched polystyrenes (HPS<sub>E</sub>, HPS<sub>AE</sub> and HPS<sub>C</sub>).

their derivatives.<sup>[38]</sup> Considering the hydrophobic nature of polystyrene, alkaline hydrolysis has to be tested under heterogeneous condition. In experiment, a THF solution of HPS<sub>E</sub> (5.0 g/L) was first mixed with a concentrated aqueous solution of NaOH (20 mol/L), and the reaction solution was sealed and vigorously stirred. The hydrolysis time dependent SEC curve was collected and analyzed. Figure 3a shows the dependence of reduced molar mass ( $M_{w,absrt=t}/M_{w,absrt=0}$ ) on hydrolysis time ( $t$ ). To our surprise, only HPS<sub>C</sub> is found to be completely intact during the whole hydrolysis process. Clearly, HPS<sub>E</sub> shows the

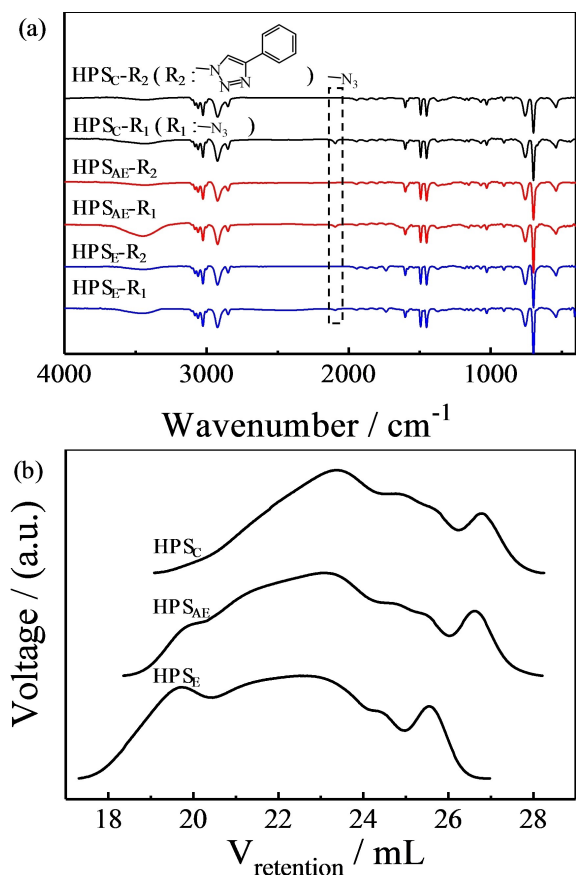


**Figure 2.** (a) The FTIR spectra of hyperbranched polystyrenes (HPS<sub>E</sub>, HPS<sub>AE</sub> and HPS<sub>C</sub>) before and after end sealing reaction. (b) SEC curves of the hyperbranched polystyrenes (HPS<sub>E</sub>, HPS<sub>AE</sub> and HPS<sub>C</sub>), where the reaction was conducted at  $T = 35\text{ }^{\circ}\text{C}$ .

highest degradation rate due to the highest hydrolysis rate of ester linkage. Figure 3b shows the evolution of SEC curve of HPS<sub>E</sub> as a function of  $t$ . The result for HPS<sub>AE</sub> is summarized in Figure S2. As displayed in Figure 3b, it is interesting to observe the transformation of tadpole-like macromonomer into linear macromonomer as  $t$  increases. At  $t = 60\text{ h}$ , a significant degradation of linear macromonomer into half fragments is observed, which actually signifies the complete consumption of ester linkage. However, such an abrupt transformation needs further investigation in future. Figure 3c shows how the ratio of  $M_{w,abs}/M_{w,app}$  and  $M_w/M_n$  change with  $t$  for HPS<sub>E</sub>, where  $M_{w,abs}$  and  $M_{w,app}$  represent the absolute and apparent molar masses of LHPs measured based on light scattering and linear calibration methods, respectively. With the increase of hydrolysis time, the  $M_{w,abs}/M_{w,app}$  ratio showed a downward trend, indicating that the degree of branching decreased, which could also reflect that HPS<sub>E</sub> was degrading. It should be noted that  $M_{w,abs,t}/M_{w,abs,t=0}$  is not a reflection of the true mass fraction of residual chemical linkages during PPM process. Seriously speaking,  $M_{w,abs,t}/M_{w,abs,t=0}$  is extremely sensitive to the degradation of chemical linkages. Therefore for HPS<sub>AE</sub>, a significant amount of ether bonds are still reserved even if  $M_{w,abs,t}/M_{w,abs,t=0} \sim 0.3$  at  $t = 48\text{ h}$ . Our observation clearly shows that the preparation of functional hyperbranched polystyrenes by using ester or aryl

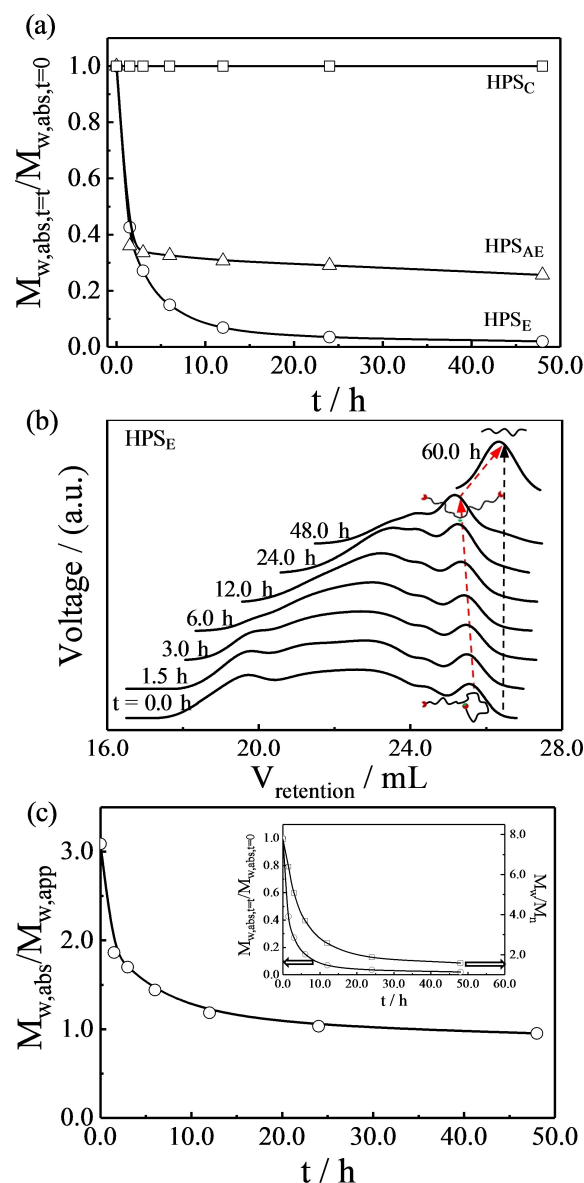


**Figure 3.** (a) Hydrolysis time ( $t$ ) dependence of reduced molar mass ( $M_{w,abs,t}/M_{w,abs,t=0}$ ) of HPS<sub>E</sub>, HPS<sub>AE</sub> and HPS<sub>C</sub>. (b) SEC curves of HPS<sub>E</sub> at different hydrolysis times. (c) Hydrolysis time ( $t$ ) dependence of the ratio of  $M_{w,abs}/M_{w,app}$  of HPS<sub>E</sub>, where the inset shows the change of  $M_{w,abs,t}/M_{w,abs,t=0}$  and  $M_w/M_n$  with  $t$  for HPS<sub>E</sub>.

ether-containing precursors is not a feasible approach due to the un-stability of chemical linkages during alkaline hydrolysis.

### 2.3. Stability of Branching Linkage under Other Typical PPM Conditions

In addition to alkaline hydrolysis, other commonly used PPM methods include TFA-promoted hydrolysis reaction,<sup>[34,35]</sup> BBr<sub>3</sub>-catalyzed methoxy-hydroxyl conversion reaction,<sup>[39]</sup> LiAlH<sub>4</sub> carbonyl reduction reaction,<sup>[40]</sup> etc. In order to intuitively explore the reaction map for the preparation of functional hyperbranched polymers, we directly studied on the stability of

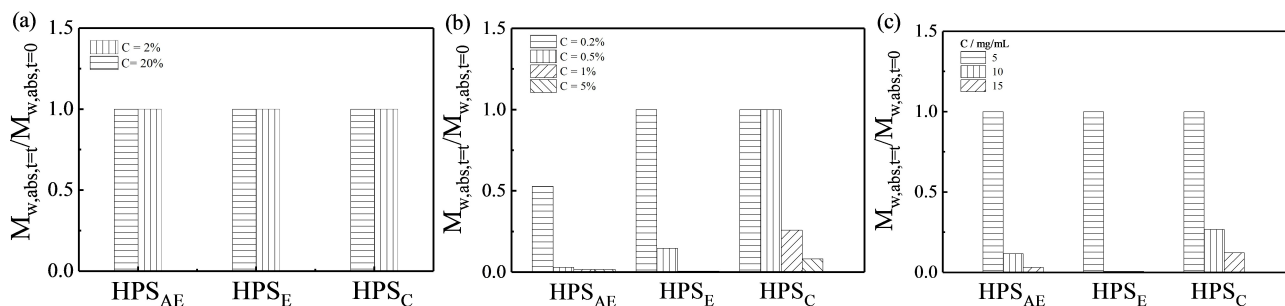


Figure 4. Changes in reduced molar mass ( $M_{w,abs,t=t}/M_{w,abs,t=0}$ ) of HPS<sub>E</sub>, HPS<sub>AE</sub> and HPS<sub>C</sub> under different concentrations of (a) TFA, (b) BBr<sub>3</sub> and (c) LiAlH<sub>4</sub>.

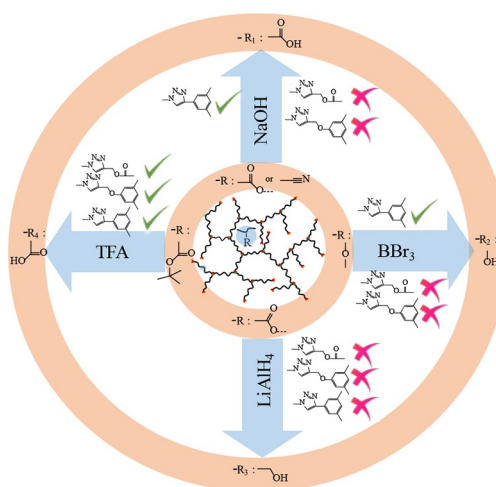
branched linkages for the above widely used PPM reactions under practical conditions. The relevant results are summarized in Figure 4, S3 and S4. As shown in Figure 4a, under different concentrations of TFA hydrolysis conditions (2% and 20% volume fraction in DCM), the experimental results show that HPS<sub>E</sub>, HPS<sub>AE</sub> and HPS<sub>C</sub> all show good stability, and  $M_{w,abs,t=t}/M_{w,abs,t=0}$  does not change with hydrolysis time ( $t$ ). It is worth mentioning that according to literature reports, in a typical TFA-promoted *t*-butyl ester-carboxyl conversion reaction, the concentration of TFA solution is usually in the range of 5~20%.<sup>[34,35]</sup> Our tests show that ester bonds, ether bonds, and triazole rings will still have good stability even at higher TFA concentrations. In other words, all three linkages can be used in related applications, such as preparing hyperbranched poly(acrylic acid) (HPAA) with hyperbranched poly(*tert*-butyl acrylate) (HPtBA) as the precursor. Different from the TFA test results, Figure 4b shows that the three linkages are more sensitive to the BBr<sub>3</sub> solution. In comparison, the stability ranking is C>E>AE. It is worth noting that there appears to be a critical concentration  $C=13.5$  g/mL (0.5% volume fraction) at which the reaction is extremely selective. For example, at  $C=13.5$  g/mL, HPS<sub>AE</sub> has been substantially degraded (Figure S3a), HPS<sub>E</sub> is partially degraded (Figure S3b), and HPS<sub>C</sub> is still intact (Figure S3c). Obviously, using hyperbranched polymers with carbon-carbon linkage as precursors, such as hyperbranched poly(2-methoxy-4-vinylphenol) (HPMVP), it is expected to prepare hyperbranched functional polymers rich in phenolic hydroxyl groups without undergoing the degradation process of branching linkage at the optimal BBr<sub>3</sub> reaction concentration.

In addition to the need of converting the ester bond to the carboxyl group, it is often necessary to convert the ester bond to the reactive hydroxyl group in real applications.<sup>[40]</sup> Recently, Zhang et al. demonstrate that reduction of polymethyl(meth)acrylate-containing block copolymers with LiAlH<sub>4</sub> provides novel poly(hydroxyisobutylene)/poly(methyl alcohol) and poly-(hydroxypropylene)/poly(allyl alcohol)-based block copolymers, and the results showed that hydroxyl-group based block copolymers can lead to extremely small domain sizes.<sup>[40]</sup> In the experiment, we gradually increased the mass concentration of lithium aluminum hydride to study the effect of its concentration effect on the linkage stability. The results are summarized in Figure 4 and S4. To our surprise, at high concentrations, all three types of branching linkage seemed to

be intolerable. In theory, the ether linkage should be inert in a reductive atmosphere, but we can see from the measured SEC curve that the mass fraction of the high molar mass region decreases significantly with the increase of reaction time in the LiAlH<sub>4</sub>/THF system. Combining theoretical knowledge<sup>[41]</sup> with our experimental observations, the results point to: triazole ring does not tolerate strong reducing reaction conditions. This result reflects disappointingly that it is difficult to directly prepare hyperbranched polyols even with hyperbranched polyesters with carbon-carbon linkage which is theoretically the most stable precursor.

### 3. Conclusion

In conclusion, based on our developed model hyperbranched system, we screened a few most popular PPM conditions, including NaOH hydrolysis reaction, TFA-promoted hydrolysis reaction, BBr<sub>3</sub>-catalyzed methoxy-hydroxyl conversion reaction, and LiAlH<sub>4</sub> carbonyl reduction reaction. Related results help establish a synthetic route map for preparing functional long-subchain hyperbranched polystyrenes and other types of branched polymers by PPM (Scheme 2) for future applications. Namely, using the guide map, we can prepare a series of



Scheme 2. Guide map for the preparation of functional long-subchain hyperbranched polystyrenes and other types of polymers by PPM.

functional hyperbranched homopolymers, including HPAA, hyperbranched poly(3,4-dihydroxystyrene) (HPDHS) and hyperbranched poly(hydroxypropylene) (HPPOH), without degrading the hyperbranched backbone. We expect that these polymers will show great potential in many important applications including biomedical research, membranes, and electrochemistry.

## Experimental Section

### Materials

Unless stated otherwise, all chemicals were obtained from commercial suppliers and were used as received. Dimethylformamide (DMF, Sinopharm, AR) was dried with anhydrous magnesium sulfate and then distilled under reduced pressure prior to use. Tetrahydrofuran (THF) and anisole from Sinopharm were distilled over CaH<sub>2</sub> just prior to use. Styrene (Sinopharm, 97%) was passed through a basic alumina column to remove inhibitor, distilled under vacuum, and stored at -20 °C. Copper(I) bromide (CuBr, Alfa, 98%) was washed with glacial acetic acid to remove soluble oxidized species, filtered, washed with diethyl ether and dried under vacuum. N,N,N',N',N'-pentamethyl-diethylenetriamine (PMDETA, Aldrich, 99%), Tris(2-(dimethylamino)ethyl)amine (Me<sub>6</sub>TREN, Aladdin, 98%), 2,2'-bipyridine (bpy, Fluka, 99%), 4,4'-di-tert-butyl-2,2'-dipyridyl (dt-bpy, Aldrich, 98%), tin(II) 2-ethylhexanoate (Sn(EH)<sub>2</sub>, Aladdin, 95%), sodium azide (NaN<sub>3</sub>, Aldrich, 99%), phenylacetylene (Aladdin, 97%), boron tribromide (BBr<sub>3</sub>, Aladdin, 1.0 M in methylene chloride), sodium hydroxide (NaOH, Sinopharm, AR), trifluoroacetic acid (TFA, Energy Chemical, 99%), lithium aluminum hydride (LiAlH<sub>4</sub>, Sinopharm, 97%) and methanol (Sinopharm, 99.8%) were used as received. Propargyl 2,2-Bis((2'-bromo-2'-methylpropanoyloxy)methyl)propionate (PBMP, ester-type)<sup>[26]</sup>, 1,3-dibromomethyl-5-propargyloxy-benzene (DBMPB, aryl-ether-type)<sup>[27]</sup> and 1,3-bis(bromomethyl)-5-ethynylbenzene (BBMEB, carbon-carbon-type)<sup>[31]</sup> was prepared according to our previously published procedure.

### Analytical Methods

NMR spectra were recorded at 300 K on a Bruker Avance III Ascend 500 (500 MHz) spectrometer with a delay time (d1) set to 8 s by using deuterated chloroform (CDCl<sub>3</sub>) as the solvent, and tetramethylsilane (TMS) as the internal standard. FTIR spectra were recorded on Bruker Tensor 27 Fourier Transform Spectrometer.

### Size Exclusion Chromatography

The molar mass distributions of macromonomer and hyperbranched polystyrene samples were characterized by a standard size-exclusion chromatography (SEC) system in our own lab,<sup>[26]</sup> where the relative number- and weight-average molar masses ( $M_n$  and  $M_w$ ) were obtained based on a conventional polystyrene calibration method (six polystyrene standards ranging from  $7.65 \times 10^2$  to  $2.21 \times 10^6$  g/mol). The absolute  $M_n$  and  $M_w$  were obtained from the measurements of a triple-detection size-exclusion chromatography (TD-SEC) system. The TD-SEC system is equipped with refractive index detector (RI), the multi-angle light scattering detector (MALS), and the viscosity detector. The instrumentation consists of a Waters 1515 Isocratic HPLC pump with 5 mm Waters Styragel columns (the efficient exclusion limit of the column system is  $5 \times 10^2 \sim 1 \times 10^7$  g/mol), a Waters 717 PLUS Autosampler, a Waters 2414 RI detector, a MALS detector (Wyatt mini-DAWN HELEOS-II)

with a scattering volume of 0.07  $\mu$ L and an 18-angle light scattering detector at a wavelength of 690 nm and 220 W power, a Wyatt Visco Star viscometer detector, and a Waters Breeze data manager. The eluent was HPLC-grade THF with a flow rate of 1.0 mL/min. Prior to injection, the sample solutions were filtered through PTFE membranes (0.45  $\mu$ m pore size). The TD-SEC system was carefully calibrated with two polystyrene standards: 1) a polystyrene standard with peak molar mass ( $M_p$ )  $\sim 3.01 \times 10^4$  g/mol was used to calibrate the detector normalization coefficient; 2) solvent toluene and a polystyrene standard with  $M_p \sim 2.21 \times 10^6$  g/mol were used to calibrate the voltage calibration constant. For quantitative study, 50  $\mu$ L of polymer solution was injected, and the polymer concentration was fixed at 15 mg/mL for all samples.<sup>[26,27,42-45]</sup>

Considering the large size (> 50 nm) and high molar mass (>  $10^6$  g/mol) of polymer samples in this study, the observation length " $1/q$ " might be much smaller than  $R_g$ , where  $q$  is the scattering vector and  $R_g$  is the radius of gyration. Thus, Berry plot was used for the extraction of molar mass and size information for all samples during the analysis of light scattering data. To perform calculations with Berry method, which is a fit to  $[KC/R(\theta)]^{1/2}$  vs  $q^2$  according to the following equation:

$$\sqrt{\frac{KC}{R_\theta}} = \frac{1}{\sqrt{M_w}}(1 + \langle R_g \rangle^2 q^2 / 6) \quad (1)$$

where  $K = 4\pi^2(dn/dc)^2/(N_A\lambda_0^4)$  and  $q = (4\pi/\lambda_0)\sin(\theta/2)$  with  $C$ ,  $dn/dc$ ,  $N_A$ , and  $\lambda_0$  being concentration of the polymer solution, the specific refractive index increment, the Avogadro's number, and the wavelength of light in a vacuum, respectively.

### Preparation of AB<sub>2</sub> Polystyrene Macromonomers

Into a 100 mL dry glass tube with a magnetic stirring bar, PBMP (0.137 g, 0.291 mmol), Me<sub>6</sub>TREN (91.4  $\mu$ L, 0.291 mmol), Sn(EH)<sub>2</sub> (113.0  $\mu$ L, 0.291 mmol) and anisole (36.4 g, 0.350 mol) were added successively. After mixing thoroughly, the polymerization tube was degassed by two freeze-vacuum-thaw cycles, CuBr (5 mg, 0.029 mmol) was then added into the frozen solution. The polymerization tube was degassed by one more freeze-vacuum-thaw cycle before flame-sealing under vacuum. The sealed tube was immersed in an oil bath at T = 80 °C. After the polymerization was carried out for 26 h, the tube was rapidly stopped in liquid nitrogen. The polymer solution was then diluted with THF and passed through a short column of neutral alumina to remove metal salt. After precipitating twice by the addition of polymer solution into methanol, the ester-type polystyrene macromonomer was obtained after being dried under vacuum at T = 45 °C overnight (yield  $\sim 5.5$  g, 94%,  $M_n = 18000$  g mol<sup>-1</sup>).

For aryl-ether-type AB<sub>2</sub> Polystyrene Macromonomers, we used DBMPB (160 mg, 0.5 mmol), 4,4'-bipyridine (bpy, 476 mg, 3.0 mmol), THF (10.4 g), St (10.4 g, 100 mmol) and CuBr (166 mg, 1 mmol), and follow the same experimental procedure as ester-type polystyrene macromonomer (yield  $\sim 3.7$  g, 85%,  $M_n = 8700$  g mol<sup>-1</sup>).

For carbon-carbon-type AB<sub>2</sub> Polystyrene Macromonomers, we used BBMEB (168 mg, 0.583 mmol), 4,4'-di-tert-butyl-2,2'-dipyridyl (dt-bpy, 469 mg, 1.749 mmol), THF (22.7 g), St (22.7 g, 0.219 mol) and CuBr (84 mg, 0.583 mmol), and follow the same experimental procedure as ester-type polystyrene macromonomer (yield  $\sim 4.1$  g, 89%,  $M_n = 7900$  g mol<sup>-1</sup>).

### Azidation Substitution Reaction

A 100 mL round-bottom flask was charged with ester-type polystyrene macromonomer (5.4 g, 0.30 mmol), DMF (60.0 mL), and  $\text{NaN}_3$  (195 mg, 3.0 mmol). The mixture was allowed to stir under nitrogen at room temperature for 24 h. The mixture was diluted with  $\text{CH}_2\text{Cl}_2$  (4.8 mL), and the insoluble inorganic salt was removed by filtration. The filtrate was precipitated into an excess of cold methanol. The sediments were redissolved in  $\text{CH}_2\text{Cl}_2$  and passed through a neutral alumina column to remove residual sodium salts, and then precipitated into an excess of methanol. After dried in a vacuum oven overnight at 45 °C, the macromonomer  $\text{PS}_E$  functionalized with one alkyne group and two azide groups was obtained (yield ~4.05 g, 75%). Following the similar protocol, the macromonomer  $\text{PS}_{AE}$  and  $\text{PS}_C$  functionalized with one alkyne group and two azide groups were synthesized.

### Preparation of Hyperbranched Samples from $\text{AB}_2$ Macromonomers via Azide-alkyne Cycloaddition Reaction

Compared with our previous protocol,<sup>[27]</sup> a slightly modified procedure was employed. Into a 25 mL dry glass tube with a magnetic stirring bar,  $\text{PS}_E$  (2.7 g, 0.15 mmol), PMDETA (63  $\mu\text{L}$ , 0.30 mmol), DMF (10 mL) were added successively. After mixing thoroughly, the polymerization tube was degassed by two freeze-vacuum-thaw cycles, and  $\text{CuBr}$  (44 mg, 0.30 mmol) was added into the frozen solution. The polymerization tube was degassed by one more freeze-vacuum-thaw cycle before sealed under vacuum. The sealed tube was immersed into an oil bath at 35 °C for 24 h. The mixture was then diluted with THF and quickly passed through a neutral alumina column. The  $\text{CuBr}$  and PMDETA were further removed from resultant hyperbranched polystyrene by the repeating precipitation with THF and methanol. Finally, the pure precipitate of hyperbranched polystyrene with ester linkages was collected by filtration and then dried under vacuum overnight at 45 °C (yield ~2.16 g, 80%). Following the similar protocol, hyperbranched polystyrene with aryl-ether and carbon-carbon linkages  $\text{HPS}_{AE}$  and  $\text{HPS}_C$  were synthesized.

### End Sealing Reaction of Hyperbranched Polymer via Azide-alkyne Cycloaddition Reaction

Into a 25 mL dry glass tube with a magnetic stirring bar, hyperbranched polystyrene with ester linkages (2 g, 9.94  $\mu\text{mol}$ ), phenylacetylene (81 mg, 0.80 mmol), PMDETA (34.5  $\mu\text{L}$ , 0.16 mmol), DMF (20 mL) were added successively. After mixing thoroughly, the polymerization tube was degassed by two freeze-vacuum-thaw cycles, and  $\text{CuBr}$  (23 mg, 0.16 mmol) was added into the frozen solution. The polymerization tube was degassed by one more freeze-vacuum-thaw cycle before sealed under vacuum. The sealed tube was immersed into an oil bath at 35 °C for 24 h. The mixture was then diluted with THF and quickly passed through a neutral alumina column. The  $\text{CuBr}$ , phenylacetylene and PMDETA were further removed from resultant hyperbranched polystyrene by the repeating precipitation with THF and methanol. Finally, the pure precipitate of hyperbranched polystyrene with ester linkages was collected by filtration and then dried under vacuum overnight at 45 °C (yield ~2.16 g, 80%). Following the similar protocol, hyperbranched polystyrene with aryl-ether and carbon-carbon linkages  $\text{HPS}_{AE}$  and  $\text{HPS}_C$  were synthesized.

### Hydrolysis of Hyperbranched Samples via NaOH

$\text{HPS}_E$  (5.0 mg, 0.02  $\mu\text{mol}$ ) was first dissolved in THF (1.0 mL), and then a saturated solution of NaOH in water (1.0 mL) was added. The

layered solution was sealed in a glass vial and stirred vigorously at room temperature for 60 h. At different time intervals, 0.1 mL of solution in organic phase was withdrawn and dried with anhydrous  $\text{Na}_2\text{SO}_4$  for SEC characterization.  $\text{HPS}_{AE}$  and  $\text{HPS}_C$  follow the same experimental procedure as  $\text{HPS}_E$ .

### Hydrolysis of Hyperbranched Samples via $\text{BBr}_3$

$\text{HPS}_E$  (5.0 mg, 0.02  $\mu\text{mol}$ ) was first dissolved in DCM (0.8 mL), and then a solution of  $\text{BBr}_3$  (25% in DCM, 0.2 mL) was added. The solution was sealed in a glass vial under nitrogen and stirred vigorously at room temperature. After 24 h, aqueous  $\text{Na}_2\text{CO}_3$  (saturated solution) was added followed by the dilution with THF. The combined organic phase was extracted, dried over  $\text{Na}_2\text{SO}_4$ , and used for SEC measurement.  $\text{HPS}_{AE}$  and  $\text{HPS}_C$  follow the same experimental procedure as  $\text{HPS}_E$ .

### Hydrolysis of Hyperbranched Samples via TFA

$\text{HPS}_E$  (5.0 mg, 0.02  $\mu\text{mol}$ ) was first dissolved in DCM (0.8 mL), and then a solution of TFA (0.2 mL) was added. The solution was sealed in a glass vial under nitrogen and stirred vigorously at room temperature. After 24 h, aqueous  $\text{Na}_2\text{CO}_3$  (saturated solution) was added followed by the dilution with THF. The combined organic phase was extracted, dried over  $\text{Na}_2\text{SO}_4$ , and used for SEC measurement.  $\text{HPS}_{AE}$  and  $\text{HPS}_C$  follow the same experimental procedure as  $\text{HPS}_E$ .

### Hydrolysis of Hyperbranched Samples via $\text{LiAlH}_4$

$\text{HPS}_E$  (5.0 mg, 0.02  $\mu\text{mol}$ ) was first dissolved in THF (1.0 mL), and then  $\text{LiAlH}_4$  (5.0 mg, 0.13 mmol) was added at 0 °C. The solution was sealed in a glass vial under nitrogen and stirred vigorously at room temperature. After 24 h, 10% aqueous solution of HCl was added followed by the dilution with THF. The combined organic phase was extracted, dried over  $\text{Na}_2\text{SO}_4$ , and used for SEC measurement.  $\text{HPS}_{AE}$  and  $\text{HPS}_C$  follow the same experimental procedure as  $\text{HPS}_E$ . Experimental Details.

## Acknowledgements

The National Natural Scientific Foundation of China Project (21774116 and 21973088) is gratefully acknowledged.

## Conflict of Interest

The authors declare no conflict of interest.

**Keywords:** post-polymerization modification · hyperbranched polymers · hydrolysis reaction · chemical stability · polystyrene

- [1] M. A. Gauthier, M. I. Gibson, H.-A. Klok, *Angew. Chem. Int. Ed.* **2009**, *48*, 48–58.
- [2] P. Theato, H.-A. Klok, *Functional polymers by post-polymerization modification: concepts, guidelines and applications*, John Wiley & Sons, **2013**.
- [3] K. A. Günay, P. Theato, H.-A. Klok, *J. Polym. Sci. Part A* **2013**, *51*, 1–28.
- [4] A. J. Inglis, S. Sinnwell, T. P. Davis, C. Barner-Kowollik, M. H. Stenzel, *Macromolecules* **2008**, *41*, 4120–4126.

- [5] S. Sinnwell, C. V. Synatschke, T. Junkers, M. H. Stenzel, C. Barner-Kowollik, *Macromolecules* **2008**, *41*, 7904–7912.
- [6] A. Kyritsis, K. Raftopoulos, M. A. Rehim, S. S. Shabaan, A. Ghoneim, G. Turkey, *Polymer* **2009**, *50*, 4039–4047.
- [7] S. Khargharia, K. Kizzire, M. D. Ericson, N. J. Baumhover, K. G. Rice, *J. Controlled Release* **2013**, *170*, 325–333.
- [8] A. Amel, L. Zhu, M. Hickner, Y. Ein-Eli, *J. Electrochem. Soc.* **2014**, *161*, F615–F621.
- [9] K. A. Chaffin, X. Chen, L. McNamara, F. S. Bates, M. A. Hillmyer, *Macromolecules*, **2014**, *47*, 5220–5226.
- [10] C. V. Amanchukwu, J. R. Harding, Y. Shao-Horn, P. T. Hammond, *Chem. Mater.* **2015**, *27*, 550–561.
- [11] K. M. Meek, Y. A. Elabd, *Macromolecules* **2015**, *48*, 7071–7084.
- [12] I. M. Heckler, J. Kesters, M. Defour, H. Penxten, B. Van Mele, W. Maes, E. Bundgaard, *J. Mater. Chem. A* **2016**, *4*, 16677–16689.
- [13] K. M. Meek, J. R. Nykaza, Y. A. Elabd, *Macromolecules* **2016**, *49*, 3382–3394.
- [14] A. D. Mohanty, S. E. Tignor, J. A. Krause, Y.-K. Choe, C. Bae, *Macromolecules* **2016**, *49*, 3361–3372.
- [15] A. M. Jazani, J. K. Oh, *Macromolecules* **2017**, *50*, 9427–9436.
- [16] T. Kim, J. Choi, H. J. Kim, W. Lee, B. J. Kim, *Macromolecules* **2017**, *50*, 6861–6871.
- [17] K. S. Lee, S. Y. Park, H. C. Moon, J. K. Kim, *J. Polym. Sci. Part A* **2017**, *55*, 427–436.
- [18] T. Liu, X. Guo, W. Liu, C. Hao, L. Wang, W. C. Hiscox, C. Liu, C. Jin, J. Xin, J. Zhang, *Green Chem.* **2017**, *19*, 4364–4372.
- [19] A. Ardana, A. K. Whittaker, K. J. Thurecht, *Macromol. Res.* **2017**, *25*, 599–614.
- [20] S. Unal, T. E. Long, *Macromolecules* **2006**, *39*, 2788–2793.
- [21] D. Liu, S. Zeng, C. Yao, A. Chen, Z. Chen, Z. Xu, *Polym. Bull.* **2009**, *63*, 213–224.
- [22] J. Han, S. Li, A. Tang, C. Gao, *Macromolecules* **2012**, *45*, 4966–4977.
- [23] S. Muthukrishnan, D. P. Erhard, H. Mori, A. H. E. Müller, *Macromolecules* **2006**, *39*, 2743–2750.
- [24] L. R. Hutchings, J. M. Dodds, S. J. Roberts-Bleming, *Macromolecules* **2005**, *38*, 5970–5980.
- [25] L. R. Hutchings, *Soft Matter* **2008**, *4*, 2150–2159.
- [26] L. Li, C. He, W. He, C. Wu, *Macromolecules* **2011**, *44*, 8195–8206.
- [27] C. He, L.-W. Li, W.-D. He, W.-X. Jiang, C. Wu, *Macromolecules* **2011**, *44*, 6233–6236.
- [28] M. Zhu, N. Hao, J. Yang, L. Li, *Polym. Chem.* **2018**, *9*, 2830–2842.
- [29] N. Hao, X. Duan, H. Yang, A. Umair, M. Zhu, M. Zaheer, J. Yang, L. Li, *Macromolecules* **2019**, *52*, 1065–1082.
- [30] N. Hao, A. Umair, M. Zhu, X. Duan, L. Li, *Macromolecules* **2019**, *52*, 6566–6577.
- [31] J. Si, N. Hao, M. Zhang, S. Cheng, A. Liu, L. Li, X. Ye, *ACS Macro Lett.* **2019**, *8*, 730–736.
- [32] L.-Z. Kong, M. Sun, H.-M. Qiao, C.-Y. Pan, *J. Polym. Sci. Part A* **2010**, *48*, 454–462.
- [33] P.-Y. Li, W.-D. He, S.-Q. Chen, X.-X. Lu, J.-M. Li, H.-J. Li, *Polym. Chem.* **2016**, *7*, 4842–4851.
- [34] H. Mori, D. C. Seng, H. Lechner, M. Zhang, A. H. E. Müller, *Macromolecules* **2002**, *35*, 9270–9281.
- [35] B.-S. Kim, H. Gao, A. A. Argun, K. Matyjaszewski, P. T. Hammond, *Macromolecules* **2009**, *42*, 368–375.
- [36] J. E. Coughlin, A. Reisch, M. Z. Markarian, J. B. Schlenoff, *J. Polym. Sci. Part A* **2013**, *51*, 2416–2424.
- [37] M. A. Cortez, W. T. Godbey, Y. Fang, M. E. Payne, B. J. Cafferty, K. A. Kosakowska, S. M. Grayson, *J. Am. Chem. Soc.* **2015**, *137*, 6541–6549.
- [38] D. A. Mortimer, *Polym. Int.* **1991**, *25*, 29–41.
- [39] Z. Yang, R. Pelton, *Macromol. Rapid Commun.* **1998**, *19*, 241–246.
- [40] W. Zhang, M. Huang, S. A. Abdullatif, M. Chen, Y. Shao-Horn, J. A. Johnson, *Macromolecules* **2018**, *51*, 6757–6763.
- [41] V. Ji Ram, A. Sethi, M. Nath, R. Pratap, in *The Chemistry of Heterocycles*, eds. V. Ji Ram, A. Sethi, M. Nath, R. Pratap, Elsevier, 2019, DOI: <https://doi.org/10.1016/B978-0-08-101033-4.00005-X>, pp. 149–478.
- [42] J. Yang, L. Li, Z. Jing, X. Ye, C. Wu, *Macromolecules* **2014**, *47*, 8437–8445.
- [43] C. He, W. D. He, L. W. Li, W. X. Jiang, J. Tao, J. Yang, L. Chen, X. S. Ge, S. Q. Chen, *J. Polym. Sci. Part A* **2012**, *50*, 3214–3224.
- [44] L. Li, X. Wang, J. Yang, X. Ye, C. Wu, *Macromolecules* **2014**, *47*, 650–658.
- [45] L. Li, Y. Lu, L. An, C. Wu, *J. Chem. Phys.* **2013**, *138*, 114908.

---

Manuscript received: May 14, 2020

Revised manuscript received: August 11, 2020